

Loophole: Timing Attacks on Shared Event Loops in Chrome

Pepe Vila^{*,†} and Boris Köpf^{*}

^{*}IMDEA Software Institute

[†]Technical University of Madrid (UPM)

{*pepe.vila, boris.koepf*}@imdea.org

Abstract

Event-driven programming (EDP) is the prevalent paradigm for graphical user interfaces, web clients, and it is rapidly gaining importance for server-side and network programming. Central components of EDP are *event loops*, which act as FIFO queues that are used by processes to store and dispatch messages received from other processes.

In this paper we demonstrate that shared event loops are vulnerable to side-channel attacks, where a spy process monitors the loop usage pattern of other processes by enqueueing events and measuring the time it takes for them to be dispatched. Specifically, we exhibit attacks against the two central event loops in Google’s Chrome web browser: that of the I/O thread of the host process, which multiplexes all network events and user actions, and that of the main thread of the renderer processes, which handles rendering and Javascript tasks.

For each of these loops, we show how the usage pattern can be monitored with high resolution and low overhead, and how this can be abused for malicious purposes, such as web page identification, user behavior detection, and covert communication.

1 Introduction

Event-driven programming (EDP) consists of defining responses to events such as user actions, I/O signals, or messages from other programs. EDP is the prevalent programming paradigm for graphical user interfaces, web clients, and it is rapidly gaining importance for server-side and network programming. For instance, the HTML5 standard [2] mandates that user agents be implemented using EDP, similarly, Node.js, memcached, and Nginx, also rely on EDP.

In EDP, each program has an *event loop* which consists of a FIFO queue and a control process (or thread) that listens to events. Events that arrive are pushed into

the queue and are sequentially dispatched by the control process according to a FIFO policy. A key feature of EDP is that high-latency (or blocking) operations, such as database or network requests, can be handled asynchronously: They appear in the queue only as events signaling start and completion, whereas the blocking operation itself is handled elsewhere. In this way EDP achieves the responsiveness and fine-grained concurrency required for modern user interfaces and network servers, without burdening programmers with explicit concurrency control.

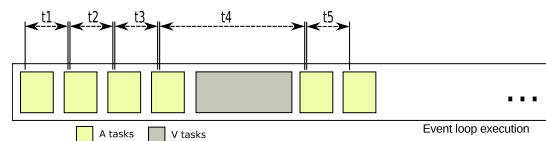


Figure 1: Shared event loop. *A* enqueues multiple short tasks and records the time at which each of them is processed. The time difference between two consecutive tasks reveals whether *V* has posted tasks in-between, and how long they took to execute.

In this paper we show that EDP-based systems are susceptible to side-channel attacks. The key observation is that event loops form a resource that can be shared between mutually distrusting programs. Hence, contention of this resource by one program can be observed by the others through variations in the time the control process takes for dispatching their events. Figure 1 illustrates such a scenario for a loop that is shared between an attacker *A* and a victim *V*.

Attacks based on observable contention of shared resources have a long history [25] and an active present [8, 27, 37]; however, attacks against shared event loops have so far only been considered from a theoretical point of view [22]. Here, we perform the first attacks against real EDP-based systems. Specifically, we target shared event loops in the two central processes of Google’s Chrome

web browser: The *host process*, whose event loop is shared between all requests for common resources, such as network and user interface; and the *renderer processes*, whose loops can be shared between Javascript tasks of different tabs or iframes.

We build infrastructure that enables us to spy on both loops from a malicious HTML page. This is facilitated by the asynchronous programming model used in both Chrome and Javascript. Asynchronous function calls trigger new tasks that are appended to the same queue, in contrast to synchronous calls which are simply pushed onto the current task’s call stack and executed without preemption, blocking the loop.

- For the event loop of the renderer we rely on the `postMessage` API, which is a Javascript feature for cross-window communication based on asynchronous callbacks. By posting messages to ourselves we can monitor the event loop with a resolution of $25\ \mu\text{s}$, with only one task in the loop at each point in time.
- For the event loop of the host process we rely on two different mechanisms: network requests to non-routable IP addresses, which enter the loop and abort very quickly, providing a resolution of $500\ \mu\text{s}$; and SharedWorkers, whose messages pass through the event loop of the host process, providing a resolution of $100\ \mu\text{s}$.

We use the information obtained using these techniques in three different attacks:

1. We show how event delays during the loading phase, corresponding to resource requests, parsing, rendering and Javascript execution, can be used to uniquely identify a web page. Figure 2 visualizes this effect using three representative web pages. While this attack shares the goal with the Memento attack [21], the channels are quite different: First, in contrast to Memento, we find that the relative ordering of events is necessary for successful classification, which motivates the use of dynamic time warping as a distance measure. Second, we show that page identification through the event loop requires only minimal training: we achieve recognition rates of up to 75% and 23% for the event loops of the renderer and host processes, respectively, for 500 main pages from Alexa’s Top sites. These rates are obtained using only one sample of each page for the training phase.

2. We illustrate how user actions in cross-origin pages can be detected based on the delays they introduce in the event loop. In particular, we mount an attack against Google OAuth login forms, in which we measure the time between keystrokes while the user is typing a password. The timing measurements we obtain from the

event loop are significantly less noisy or require less privileges than from other channels [20, 38, 18].

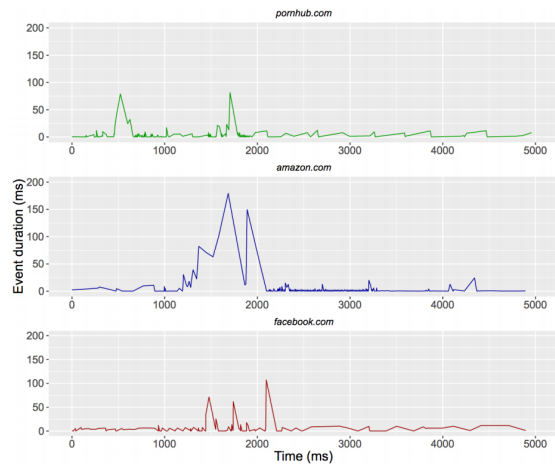


Figure 2: Delays observed while loading different web pages, by an attacker tab sharing the renderer process. Horizontal axis depicts elapsed real time, vertical axis depicts time taken by the event loop for processing the tasks inserted by the attacker. All pages are clearly distinguishable, both by the human eye and by classification techniques.

3. We demonstrate that shared event loops can be used to transmit information between cross-origin pages. Specifically, we implement a covert channel with a bandwidth of 200 bit/s through the renderer’s main thread event loop, and another one working cross-processes of 5 bit/s.

Our attacks show that event loops can be successfully spied on even with simple means. They work under the assumption that event loops behave as FIFO queues; in reality, however, Chrome’s event loop has a more sophisticated structure, relying on multiple queues and a policy-based scheduler. We believe that this structure can be leveraged for much more powerful attacks in the future.

2 Isolation Policies and Sharing of Event Loops in Chrome

In this section we revisit the same origin policy and its variants. We then discuss the relationship of these policies with the Chrome architecture, where we put a special focus on the way in which event loops are shared.

2.1 Same Origin Policy

The Same-Origin Policy (SOP) is a central concept in the web security model: The policy restricts scripts on a

web page to access data from another page if their origins differ. Two pages have the same origin if protocol, port and host are equal.

The demand for flexible cross-origin communication has triggered the introduction of features such as domain relaxation, the `postMessage` API, Cross-origin Resource Sharing (CORS), Channel Messaging, Suborigins, or the Fetch API. This feature creep comes with an increase in browser complexity and attack surface, which has motivated browser vendors to move towards more robust multi-process architectures.

2.2 Overview of the Chrome Architecture

The Chrome architecture is segmented into different operating system processes. The rationale for this segmentation is twofold: to isolate web content from the host [6], and to support the enforcement of origin policies by means of the OS [30]. For achieving this segmentation, Chrome relies on two processes:

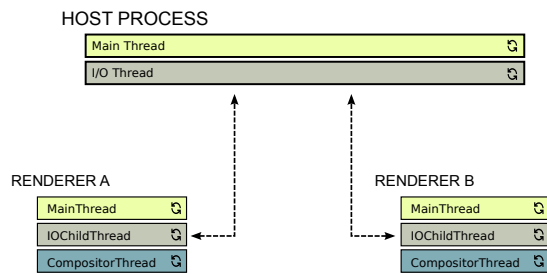


Figure 3: Overview of Chrome’s architecture.

The *host process* runs the top-level browser window. It has access to system resources such as network, file system, UI events, etc., which it manages on behalf of the unprivileged renderer processes. The host process runs several threads; the most relevant ones are:

- the `CrBrowserMain` thread, which handles, e.g., user interaction events, and
- the `IOThread`, which handles, e.g., IPC, network stack, and file system.

The *renderer processes* are sandboxed processes responsible for parsing, rendering and Javascript execution. Communication with the host process is done via an inter-process communication (IPC) system based on message passing. Each renderer runs several threads; the most relevant ones are:

- the `MainThread` where resource parsing, style calculation, layout, painting and non-worker Javascript runs,
- the `IOChildThread`, which handles IPC communication with the host process, and

- the `CompositorThread`, which improves responsiveness during the rendering phase by allowing the user to scroll and see animations while the main thread is busy, thanks to a snapshot of the page’s state.

Each of the threads in the host and renderer processes maintains at least one event loop that is largely a FIFO queue. Inter-thread and inter-process communication are carried out via message passing through these queues. We next discuss scenarios where pages of different origin can share the event loops of host and renderer processes. In Section 3 we show how this sharing can be exploited for eavesdropping.

2.3 Sharing in the Renderer Processes

Chrome supports different policies that govern how web applications are mapped to renderer processes, and that influence whether or not event loops are shared.

The default policy is called *process-per-site-instance*. It requires using a dedicated renderer process for each instance of a site. Here, a *site* is defined as a registered domain plus a scheme. For example, `https://docs.google.com` and `https://mail.google.com:8080` are from the same site – but not from the same origin, as they differ in subdomain and port. A *site instance* is a collection of pages from the same site that can obtain references to each other (e.g., one page opened the other in a new window using Javascript).

The other supported policies are more permissive. For example, the *process-per-site* policy groups all instances of a site in the same renderer process, trading robustness for a lower memory overhead. The *process-per-tab* policy dedicates one renderer process to each group of script-connected tabs. Finally, the *single-process* policy lets both the host and renderer run within a single OS process (only used for debugging purposes).

Even in the restrictive default *process-per-site-instance* policy, there are some situations that force Chrome to host documents from different sites in the same renderer process, causing them to share the event loop:

- Iframes are currently hosted in the same process as their parent.
- Renderer-initiated navigations such as link clicks, form submissions, and scripted redirections will reuse the same renderer as the origin page.
- When the number of renderer processes exceeds a certain threshold, Chrome starts to reuse existing renderers instead of creating new ones.

On (64-bit) OSX and Linux, the threshold for reusing renderers is calculated by splitting half of the physical

RAM among the renderers, under the assumption that each consumes 60MB.¹ In our experiments, on a machine with 4GB of RAM we could spawn 31 new tabs before any renderer was shared, whereas on a machine with 8GB of RAM we observed a threshold of approximately 70 renderers. There is no apparent grouping policy for the pages that can share a process when this threshold is exceeded, except for tabs in Incognito mode not being mixed up with “normal” tabs. In particular, we do not observe any preference for similar origins, same sites, or secure versus insecure pages. In fact, even filesystem pages (loaded with `file://`) can co-reside with an arbitrary HTTP site.

2.4 Sharing in the Host Process

The Chrome sandbox restricts access of renderers to privileged actions. In particular, renderers have to communicate with the host process for network requests or user input. The corresponding messages of all renderers pass through the event loop of the host process’ I/O thread.

We illustrate this communication using two different examples: how user actions flow from the host to the corresponding renderer process, and conversely, how network requests flow from a renderer to the host process.

- *UI flow*: User actions such as mouse movements or clicks enter the browser through the main thread of the host process. The host main thread communicates the user event to the corresponding renderer by message passing between their I/O event loops, and the render acknowledges the receipt of this message. Even events with no Javascript listeners occupy the event loop of the renderer’s main thread for a measurable interval.
- *Net stack*: Chrome’s net stack is a complex cross-platform network abstraction. Any network request by a renderer is passed to the I/O thread of the host process, which forwards it to a global resource dispatcher that will pass it to a worker to fulfill the request. This worker will open a connection, if necessary, and request the resource. After the request is done, the response headers are received and sent back to the renderer process, which will respond with an ACK after reading. Finally, the body is received and the corresponding callbacks are triggered.

¹On Android there is no threshold since the OS suspends idle processes.

3 Eavesdropping on Event Loops in Chrome

In this section we describe how to violate the SOP by eavesdropping on the event loops of Chrome’s host and renderer processes. For each of these processes, we describe potential threat scenarios and present a simple HTML page executing Javascript that can be used for spying. We then present our monitoring tool to visualize the event loops of the browser.

3.1 The Renderer Process Event Loop

3.1.1 Threat Scenarios

There are several scenarios in which an adversary site *A* can share the event loop of the renderer’s main thread with a victim site *V*. These scenarios are based on Chrome’s policy for mapping sites to renderers, see Section 2.3. We give two examples:

- *Malicious advertisement*. In this scenario, *A* runs as an advertisement iframed in *V*. The SOP protects *V*’s privacy and integrity by logically isolating both execution environments. However, *A*’s iframe is able to execute Javascript on *V*’s event loop, enabling it to gather information about the user behavior in *V*.
- *Keylogger*. In this scenario, *A* pops up a login form to authenticate its users via *V*’s OAuth. Because the operation does not ask for special privileges and the password is never sent to *A*, the victim could trust it and fill the form. Meanwhile, *A*’s page monitors keystroke timings (see Section 4.2), which can be used for recovering user passwords [32].

3.1.2 Monitoring Techniques

To monitor the renderer’s event loop it is sufficient to continuously post asynchronous tasks and measure the time interval between subsequent pairs of events. We measure the monitoring resolution in terms of the interval between two subsequent measurement events on an otherwise empty loop.

The most common way of posting asynchronous tasks programmatically in Javascript is `setTimeout`. However, the resolution can be more than 1000 ms for inactive tabs, rendering this approach useless for the purpose of spying. To increase the resolution, we instead use the `postMessage` API for sending asynchronous messages to ourselves.

The code in Listing 1 shows how this is achieved. The call to `performance.now()` in line 2 of the function `loop` returns a high-resolution timestamp that is saved as described below. The call to `self.postMessage(0, '*')` in line 3 posts message

```
1 function loop() {
2     save(performance.now())
3     self.postMessage(0, '*')
4 }
5 self.onmessage = loop
6 loop()
```

Listing 1: Javascript code to monitor the main thread’s event loop with the `postMessage` API.

“0” into the renderer’s event loop, where the second argument “*” indicates no restriction on the receiver’s origin. Line 5 registers the function `loop` as an event listener, which enables it to receive the messages it has posted. This causes `loop` to recursively post tasks, while keeping the render responsive since other events are still being processed.

In order to minimize the noise introduced by the measurement script itself, the function `save` in line 2 uses a pre-allocated typed array (`Float64Array`) to store all the timing measurements. Contrary to normal Javascript’s sparse arrays, typed arrays avoid memory re-allocations and thus noisy garbage collection rounds, see below. With that we achieve an average delay between two consecutive tasks of around $25\mu\text{s}$ on our target machine. This resolution is sufficient to identify even short events. For example, a single mouse movement event (without explicit event listener) consumes around $100\mu\text{s}$.

3.1.3 Interferences

In modern browsers there are several sources of noise that affect measurement precision, beside the obvious effect of the underlying hardware platform and OS. They include:

- *Just-in-time compilation (JIT)*. JIT can trigger code optimization or deoptimization, in the case of Chrome by the Crankshaft and Turbofan compilers, at points in time that are hard to predict. For our measurements we rely on a warm-up phase of about 150 ms to obtain fully optimized code.
- *Garbage collection (GC)*. In the case of V8, GC includes small collections (so-called *scavenges*) and major collections. Scavenges are periodical and fast ($< 1\text{ ms}$); but major collections may take $> 100\text{ ms}$, distributed into incremental steps. In our data, scavenges are easily identifiable due to their periodicity, while major collections could be spotted due to their characteristic size. On some browsers, such as Microsoft’s Internet Explorer, GC rounds can be triggered programmatically, which helps to eliminate noise from the measurements enabling more precise attacks [11].

While all of these features reduce the effectiveness of our attacks, it is interesting to think of them as potential side-channels by themselves. For example, observable GC and JIT events can reveal information about a program’s memory and code usage patterns, respectively [29].

3.2 The Host Process Event Loop

3.2.1 Threat Scenarios

The Chrome sandbox ensures that all of the renderer’s network and user interaction events pass through the host process’ I/O event loop, see Section 2.4. We describe two threat scenarios where this could be exploited.

- *Covert channel*. Pages of different origins running in different (disconnected) tabs can use the shared event loop to implement a covert channel, violating the browser’s isolation mechanisms. This will work even if one (or both) pages run in incognito mode. This channel can be used for tracking users across sessions, or to exfiltrate information from suspicious web pages without network traffic.
- *Fingerprinting*. A tab running a rogue page of *A* can identify which pages are being visited by the user in other tabs by spying on the shared event loop. Detecting the start of a navigation is facilitated by the fact that the I/O thread blocks for a moment when the user types in a URL and presses enter.

3.2.2 Monitoring Techniques

There are many ways to post asynchronous tasks into the event loop of the host process; they differ in terms of the resolution with which they enable monitoring the event loop and the overhead they imply. Below we describe two of the techniques we used.

Network Requests. The first technique is to use network requests to systematically monitor the event loop of the I/O thread of the host process. A valid network request may take seconds to complete, with only the start and end operations visible in the loop, which provides insufficient resolution for monitoring.

To increase the resolution, we make use of *non-routable* IP addresses. The corresponding requests enter the I/O thread’s event loop, are identified as invalid within the browser, and trigger the callback without any DNS resolution or socket creation. This mechanism provides a monitoring resolution of $500\mu\text{s}$ and has the additional benefit of being independent from network noise.

Listing 2 shows the code of our monitoring procedure. We rely on the Javascript Fetch API for posting the network requests. The Fetch API provides an interface for fetching resources using *promises*, which are ideal to

manage asynchronous computations thanks to their simple syntax for handling callbacks. In line 2 we request and save a high-resolution timestamp. In line 3 we request a non-routable IP address, and set the rejection callback of the promise to self, to recursively run when the request fails.

```
1 function loop() {
2   save(performance.now())
3   fetch(new Request('http://0/')).
4     catch(loop)
5 }
6 loop()
```

Listing 2: Javascript code to monitor the host’s I/O thread using network requests.

Shared Workers. The second technique relies on web workers, which is a mechanism for executing Javascript in the background. Web workers that are *shared* between multiple pages are usually implemented in a dedicated OS process; this means they communicate via IPC and, therefore, can be used to spy on the I/O thread of the host process. This mechanism provides a monitoring resolution of $100\mu s$. Listing 3 shows the code of our worker-

```
1 onconnect = function reply(e) {
2   let port = e.ports[0]
3   port.onmessage = function() {
4     port.postMessage(0)
5   }
6 }

1 const w = new SharedWorker('pong.js')
2 function loop() {
3   save(performance.now())
4   w.port.postMessage(0)
5 }
6 w.port.onmessage = loop
7 loop()
```

Listing 3: Javascript code to monitor the host’s I/O thread using SharedWorkers. The first snippet is the worker’s ‘pong.js’ file. Second snippet is the Javascript code that monitors the I/O thread by communicating with the worker.

based monitoring procedure. The first snippet defines the worker’s job, which consists in replying to each received message. In the second snippet, we register the worker in line 1. In lines 2-7 we record a timestamp and recursively send messages to the worker, analogous to Listing 1. As a result, we measure the round-trip time from the page to the worker, which reflects the congestion in the I/O event loop. Note that one can further increase the measurement resolution by recording the time in each endpoint and merging the results.

3.2.3 Interferences

There are many different sources of noise and uncertainty in the I/O thread of the host process. The most notable ones include the interleaving with the host’s main thread and the messages from other renderers, but also the GPU process and browser plugins. While these interferences could potentially be exploited as side channels, the noise becomes quickly prohibitive as the loop gets crowded.

3.3 The LoopScan Tool

We implement the eavesdropping techniques described in Sections 3.1 and 3.2 in a tool called LoopScan, which enables us to explore the characteristics of the side channel caused by sharing event loops. LoopScan is based on a simple HTML page that monitors the event loops of the host and renderer processes. It relies on the D3.js framework, and provides interactive visualizations with minimap, zooming, and scrolling capabilities, which facilitates the inspection of traces. For example, Figure 8 is based on a screenshot from LoopScan.

LoopScan’s functionality is in principle covered by the powerful Chrome Trace Event Profiling Tool (about:tracing) [3], which provides detailed flame graphs for all processes and threads. However, LoopScan has the advantage of delivering more accurate timing information about event-delay traces than the profiler, since loading a page with the Trace Event Profiling tool severely distorts the measurements. LoopScan source is publicly available at <https://github.com/cgvwzq/loopscan>.

4 Attacks

In this section we systematically analyze the side channel caused by sharing event loops in three kinds of attacks: a page identification attack, an attack where we eavesdrop on user actions, and a covert channel attack. For all attacks we spy on the event loops of the renderer and the host processes, as described in Sections 3.1 and 3.2. We performed these attacks over the course of a year, always using the latest stable version of Chrome (ranging from v52-v58). The results we obtain are largely stable across the different versions.

4.1 Page identification

We describe how the event-delay trace obtained from spying on event loops can be used for identifying web-pages loaded in other tabs. We begin by explaining our data selection and harvesting process and the chosen analysis methods, then we describe our experimental setup and the results we obtain.

4.1.1 Sample Selection

We start with the list of Alexa Top 1000 sites, from which we remove duplicates. Here, duplicates are sites that share the subdomain but not the top-level domains (e.g., “google.br” and “google.com”) and that are likely to have similar event-delay traces. From the remaining list, we randomly select 500 sites as our sample set. This reduction facilitates a rigorous exploration of the data and the parameter space.

4.1.2 Data Harvesting

We visit each page in the sample set 30 times for both the renderer and the host process, to record traces of event-delays during the loading phase.

The event-delay traces for the *renderer process* consist of 200.000 data items each. On our testing machine, the measurement resolution (i.e. the delay between two subsequent measurement events on an otherwise empty loop) lies at approximately $25\mu s$. That is, each trace captures around 5 seconds ($200.000 \cdot 25\mu s = 5s$) of the loading process of a page in the sample set.

The event-delay traces for the *host process* consist of 100.000 data items each. The measurement resolution lies in the range of $80 - 100\mu s$, i.e. each trace captures around 9s of the loading process of a page.

We automate the harvesting procedure for the renderer process as follows:

1. Open a new tab via
`target = window.open(URL, '_blank');`²
2. Monitor the event loop until the trace buffer is full
3. Close the tab
4. Send the trace to the server
5. Wait 5 seconds and go to 1 with next URL

The harvesting procedure for the host process differs only in that we use the `rel="noopener"` attribute in order to spawn a new renderer.

We conducted measurements on the following three machines:

1. Debian 8.6 with kernel 3.16.0-4-amd64, running on an Intel i5 @ 3.30GHz x 4 with 4 GB of RAM, and Chromium v53;
2. Debian 8.7 with kernel 3.16.0-4-amd64, running on an Intel i5-6500 @ 3.20GHz x 4 with 16 GB of RAM, and Chromium v57; and
3. OSX running on a Macbook Pro 5.5 with Intel Core 2 Duo @ 2.53GHz with 4 GB of RAM, and Chrome v54.

²Note that this requires disabling Chrome’s popup blocker from “chrome://settings/content”.

We measure the timing on a Chrome instance with two tabs, one for the spy process and the other for the target page. For the renderer process, we gather data on all machines; for the host process on (2) and (3). Overall, we thus obtain five corpora of 15.000 traces each.

4.1.3 Classification

Event Delay Histograms. Our first approach is to cluster the observed event delays around k centers, and to transform each trace into a histogram that represents the number of events that fall into each of the k classes. We then use the Euclidean distance as a similarity measure on the k -dimensional signatures.

This approach is inspired by the notion of memprints in [21]. It appears to be suitable for classifying event-delay traces obtained from event loops because, for example, static pages with few external resources are more likely to produce long events at the beginning and stabilize soon, whereas pages with Javascript resources and animations are likely to lead to more irregular patterns and produce a larger number of long delays. Unfortunately, our experimental results were discouraging, with less than a 15% of recognition rate in small datasets.

Dynamic Time Warping. Our second approach is to maintain temporal information about the observed events. However, the exact moments at which events occur are prone to environmental noise. For example, network delays will influence the duration of network requests and therefore the arrival of events to the event loop. Instead, we focus on the relative ordering of events as a more robust feature for page identification.

This motivates the use of *dynamic time warping (DTW)* [7] as a similarity measure on event-delay traces. DTW is widely used for classifying time series, i.e. sequences of data points taken at successive and equally spaced points in time. DTW represents a notion of distance that considers as “close” time-dependent data of similar shape but different speed, i.e. DTW is robust to horizontal compressions and stretches. This is useful, for example, when one is willing to assign a low distance score to the time series “abc” and “abbbbc”, insensitive to the prolonged duration of “b”. Formally, DTW compares two time series: a *query*, $X = (x_1, \dots, x_n)$, and a *reference*, $Y = (y_1, \dots, y_m)$. For that we use a non-negative distance function $f(x_i, y_j)$ defined between any pair of elements x_i and y_j . The goal of DTW is to find a matching of points in X with points in Y , such that (1) every point is matched, (2) the relative ordering of points in each sequence is preserved (monotonicity), (3) and the cumulative distance (i.e. the sum of the values of f) over all matching points is minimized. This matching is called a

warping path, and the corresponding distance is the *time warping distance* $d(X, Y)$.

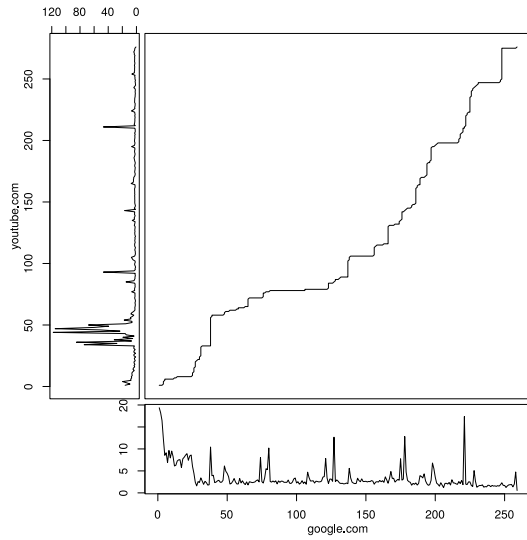


Figure 4: The path in the upper right square represents the optimal alignment between points in the time series corresponding to 'google.com' (horizontal axis) with points in the time series of 'youtube.com' (vertical axis).

Figure 4 visualizes a warping path between the time series corresponding to event-delay traces observed while loading different webpages.

4.1.4 Speed-up Techniques

Unfortunately, the time required for computing $d(X, Y)$ is quadratic in the length of the input sequences and does not scale up to the raw data obtained in our measurements. We rely on two kinds of speed-up techniques, one at the level of the data and the other at the level of the algorithm:

At the level of data, we reduce the dimension of our data by applying a basic sampling algorithm: We split the raw trace into groups of measurements corresponding to time intervals of duration P , and replace each of those groups by one representative. This representative can be computed by summing over the group, or by taking its average, maximum or minimum. The *sum* function generally yields the best results among different sampling functions and is the one that we use onwards. Sampling reduces the size of the traces by a factor of P/t , where t is the average duration of an event delay. Figure 5 shows two plots with the raw data taken from a renderer's main thread loop, and its corresponding time series obtained after sampling.

At the algorithmic level, we use two sets of techniques for pruning the search for the optimal warping path, namely windowing and step patterns [15].

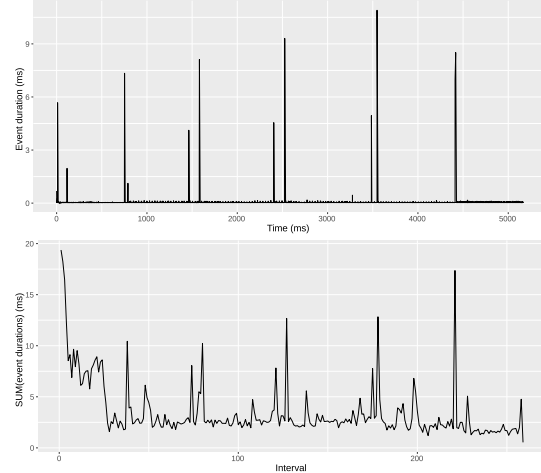


Figure 5: The top figure represents a raw trace of 200.000 time measurements from the renderer's main thread extracted while loading "google.com". The bottom figure displays the same data after being converted into a time series with $P = 20$ ms, i.e. using only 250 data points. The difference in the height of the peaks is due to the accumulation of small events in the raw data, which are not perceptible in the top figure.

- *Windowing* is a heuristic that enforces a global constraint on the envelope of the warping path. It speeds up DTW but will not find optimal warping paths that lie outside of the envelope. Two well-established constraint regions are the *Sakoe-Chiba band* and the *Itakura parallelogram*, see Figure 6.

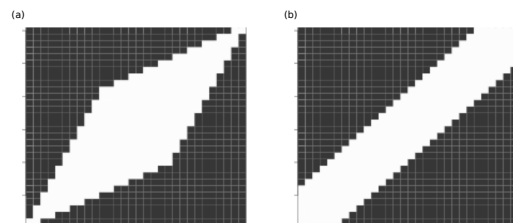


Figure 6: A global window constraint defines an envelope limiting the search space for optimal warping paths: (a) Itakura parallelogram, and (b) Sakoe-Chiba band.

- *Step patterns* are a heuristic that puts a local constraint on the search for a warping path, in terms of restrictions on its slope. In particular, we rely on three well-known step patterns available in R. Intuitively, the *symmetric1* pattern favors progress close to the diagonal, the *symmetric2* pattern allows for arbitrary compressions and expansions, and the *asymmetric* forces each point in the reference to be used only *once*.

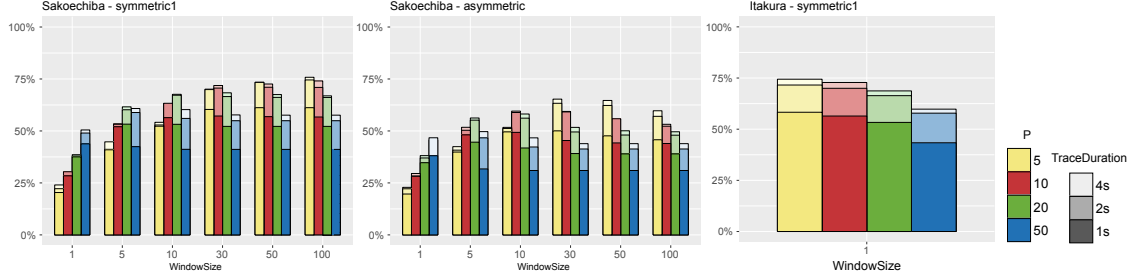


Figure 7: Web page identification performance after tuning with traces from the renderer on Linux machine (1). Effect of P , $traceDuration$, and $windowSize$, with three combinations of $stepPattern$ and $windowType$.

4.1.5 Parameter tuning

The possible configurations of the techniques presented in Section 4.1.4 create a large parameter space, see Table 1 for a summary.

Parameter	Values	Description
$traceDuration$	1000, 2000, 4000	Trace duration (ms)
P	5, 10, 20, 50	Sampling interval (ms)
$windowType$	<i>itakura</i> , <i>sakoechiba</i>	Window constraint
$windowSize$	1, 5, 10, 30, 50, 100	Window size
$stepPattern$	<i>symmetric1</i> , <i>symmetric2</i> , <i>asymmetric</i>	Step pattern

Table 1: List of parameters tuned for optimizing web page identification

We systematically identify the optimal parameter configuration for each event loop on each machine. To avoid overfitting, we divide our dataset of 30 traces (per page, loop, and machine) into 15 traces for tuning and 15 for cross-validation. For each parameter configuration we perform a lightweight version (with 3 rounds) of the evaluation phase described in Section 4.1.6. Figure 7 visualizes an extract of the results we obtain for the renderer process of the Linux (1) machine. The tuning phase yields the following insights:

- The optimal parameters depend on the loop but appear to be stable across machines.
- Measuring the loading phase during 2 seconds is sufficient for recognition of a webpage; the gain in recognition from using longer traces is negligible.
- P and $windowSize$ are the parameters with the biggest impact on the recognition rate. However, they also have the biggest impact on the computational cost (the optimal choice being most expensive one).
- The combination of $stepPattern = symmetric1$ and $windowType = sakoechiba$ generally yields the best results.

4.1.6 Experimental Results

We evaluate the performance of page identification through the shared event loops of host and renderer pro-

cesses on each individual machine, as well as through the renderer process across two different machines.

To this end, we select the top configuration for each corpus from the tuning phase and carry out a 10-fold cross-validation. In each of the 10 rounds, we partition the validation set into a training set that contains *one* trace of each page, and a testing set that contains *three* different (out of the 14 available) traces of each page. For each of the traces in the testing set, we compute the set of k closest matches in the training set according to the time warping distance.

We measure performance in terms of the k -match rate, which is the percentage of pages in the testing set for which the true match is within the set of k closest matches. We abbreviate the 1-match rate by *recognition rate*, i.e. the percentage of pages where the best match is the correct one. The result of the cross-validation is the average k -match rate over all 10 rounds.

Table 2 summarizes our experiments. We highlight the following results:

		k			
		1	3	5	10
(1)	Renderer	76.7 %	86.7 %	88.8 %	91.1 %
		<i>sym1, sakoe, P = 5, windowSize = 100</i>			
(2)	Renderer	58.2 %	68.6 %	71.8 %	75.1 %
		<i>sym1, sakoe, P = 5, windowSize = 100</i>			
	I/O host	16.2 %	23.2 %	27.9 %	36.1 %
		<i>sym1, sakoe, P = 20, windowSize = 30</i>			
(3)	Renderer	61.8 %	74.5 %	78.4 %	83.1 %
		<i>sym1, sakoe, P = 5, windowSize = 100</i>			
	I/O host	23.48 %	32.9 %	38.1 %	46.6 %
		<i>sym1, sakoe, P = 20, windowSize = 30</i>			

Table 2: 10-fold cross-validation results on different machines and different event loops, with the best configuration after tuning. Machines (1) and (2) refer to the Linux desktops, (3) to the OSX laptop, as described in Section 4.1.2.

- We can correctly identify a page by spying on the renderer from (1) in up to 76.7% of the cases, and cor-

rectly narrow down to a set of 10 candidates in up to 91.1% of the cases.

- We can correctly identify a page though the host process from (3) in up to 23.48% of the cases, and narrow down to a set of 10 candidates in up to 46.6% of the cases.

- We stress that these recognition rates are obtained using a *single* trace for training.

- Recognition is easier through the renderer than through the host. This is explained by the difference in noise and measurement resolution, see Section 3.2.3. Furthermore, most operations on the host only block the I/O thread while signaling their start and completion, whereas the renderer is blocked during the entire execution of each Javascript task.

- We observe different recognition rates on different machines. However the homogeneity in hardware and software of Macbooks facilitate reuse of training data across machines, which may make remote page identification more feasible.

- We obtain recognition rates below 5% for recognition across machines (1) and (3). A reason for this poor performance is that events on the OSX laptop often take 2x-5x more time than on the Linux desktop machine. This difference is reflected in the height of the peaks (rather than in their position), which is penalized by DTW. Normalizing the measurements could improve cross-machine recognition.

The code and datasets used for tuning and cross-validation are available as an R library at <https://github.com/cgvwzq/rlang-loop-hole>.

4.1.7 Threats to Validity

We perform our experiments in a closed-world scenario with only 2 tabs (the spy and the victim) sharing an event loop. In real world scenarios there can be more pages concurrently running the browser, which will make detection harder. The worst case for monitoring the host process occurs when a tab performs streaming, since the loop gets completely flooded. The renderer’s loop, however, is in general more robust to noise caused by other tabs in the browser.

On the other hand, our attacks do not make any use of the pages’ source code or of details of Chrome’s scheduling system with priority queues, the GC with periodic scavenges, or the frame rendering tasks. We believe that taking into account this information can significantly improve an adversary’s eavesdropping capabilities and enable attacks even in noisy, open-world scenarios.

4.2 Detecting User Behavior

In this section we show that it is possible to detect user actions performed in a cross-origin tab or iframe, when the renderer process is shared. We first describe an attack recovering the inter-keystroke timing information against Google’s OAuth login forms, which provides higher precision than existing network-based attacks [32].

4.2.1 Inter-keystroke Timing Attack on Google’s OAuth login form

Many web applications use the OAuth protocol for user authentication. OAuth allows users to login using their identity with trusted providers, such as Google, Facebook, Twitter, or Github. On the browser, this process is commonly implemented as follows:

1. A web application *A* pops up the login form of a trusted provider *T*;
2. User *V* types their (name and) password and submits the form to *T*;
3. *T* generates an authorization token.

Because the window of the login form shares the event loop with the opener’s renderer, a malicious *A* can eavesdrop on the keystroke events issued by the login form.

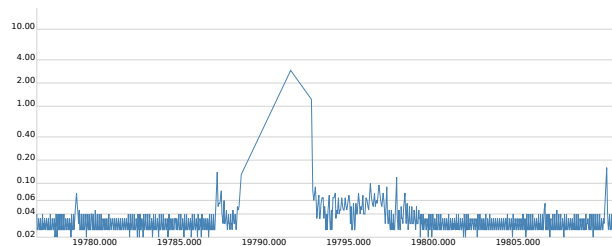


Figure 8: Delay pattern generated by a keystroke in the Google OAuth login form, measured across origins on Chrome Canary v61 on OSX. The two consecutive delays of approx. 2ms each, correspond to keydown and keypress event listeners.

Figure 8 depicts the event-delay trace of a keystroke as seen by an eavesdropper on the renderer’s event loop. The trace contains two characteristic consecutive delays, caused by the keydown and keypress event listeners. We use this observation to identify keystrokes, by scanning the event-delay trace for pairs of consecutive delays that are within a pre-defined range, forgoing any training or offline work. Listing 4 contains the script that performs this operation. We define 0.4 ms as a lower bound, and 3.0 ms as an upper bound for the range. We chose this threshold before gathering the data, by manual inspection of a few keystroke events. Note that this calibration could be done automatically, based on the victim’s interactions with a page controlled by an attacker.

```

1  const L = 0.4, U = 3.0, keys = []
2
3  for(let i=1; i<trace.length-1; i++){
4      let d1 = trace[i] - trace[i-1],
5          d2 = trace[i+1] - trace[i]
6
7      if (L<d1<U && L<d1<U){
8          keys.push(trace[i])
9      }
10 }

```

Listing 4: Pseudo-Javascript code to detect keystrokes in a trace of timestamps gathered by the code in Listing 1. We classify a timestamp as a keystroke if the differences to the previous and subsequent timestamps ($d1$ and $d2$) are both in a predefined range.

4.2.2 Experimental Evaluation

To evaluate the effectiveness of this attack, we have implemented a malicious application A that extracts the inter-keystroke timing information from a user V logging-in via Google’s OAuth. The focus of our evaluation is to determine the accuracy with which keystroke timings can be measured through the event loop. A full keystroke recovery attack is out of scope of this paper; for this refer to [32].



Figure 9: Experimental setup for evaluating effectiveness of automatic, cross-renderer keystroke detection.

We simulate an inter-keystroke timing attack in 4 steps, which are described below and illustrated in Figure 9.

1. A Selenium³ script acting as V navigates to A , clicks on the login button (which pops up Google’s OAuth login form), types a password, and submits the form.
2. Meanwhile, the attacker A monitors the main thread’s event loop using the attack described in Section 4.2.1.

³Selenium (<http://www.seleniumhq.org/>) is a cross-platform testing framework for web applications that provides capabilities for programmatically navigating to web pages and producing user input.

3. V and A send to the server the timestamps of the *real* and the *detected* keystrokes, respectively.
4. We compute the accuracy of the detected keystrokes, where we take the timestamps of the real keystrokes as ground truth. Matching the timestamps requires taking into account the delay (6 – 12 ms on our machine) between Selenium triggering an event, and Chrome receiving it.

We use as inter-keystroke timings random delays uniformly drawn from 100 – 300 ms. This choice is inspired by [20], who report on an average inter-keystroke delay of 208 ms. Using random delays is sufficient for evaluating the accuracy of eavesdropping on keystrokes, but it obviously does not reveal any information about the password besides its length.

4.2.3 Experimental Results

We perform experiments with 10,000 passwords extracted from the RockYou dataset, where we obtain the following results:

- In 91.5% of the cases, our attack correctly identifies the length of a password.⁴ In 2.2% of the cases, the attack misses one or more characters, and in 6.3% of the cases it reports spurious characters.
- For the passwords whose length was correctly identified, the average time difference between a true keystroke and a detected keystroke event is 6.3ms, which we attribute mostly to the influence of Selenium. This influence cancels out when we compute the average difference between a true inter-keystroke delay and a detected inter-keystroke delay, which amounts to 1.4 ms. The noise of these measurements is low: We observe a standard deviation of 6.1 ms, whereas the authors of [20] report on 48.1 ms for their network based measurements.

Overall, our results demonstrate that shared event loops in Chrome enable much more precise recovery of keystroke timings than network-based attacks. Moreover, this scenario facilitates to identify the time when keystroke events enter the loop (from popping-up to form submission), which is considered to be a major obstacle for inter-keystroke timing attacks on network traffic [20].

Keystroke timing attacks based on monitoring *procs* [38] or CPU caches [18] can extract more fine-grained information about keystrokes, such as containment in a specific subsets of keys. However, they require filesystem access or are more susceptible to noise, due to the resource being shared among all processes in the system. In contrast, our attack enables targeted eavesdropping without specific privileges.

⁴We configured Selenium to atomically inject characters that would require multiple keys to be pressed.

4.2.4 Open Challenges for Recognizing User Events

We conclude by discussing two open challenges for recognizing user events, namely the detection of user events beyond keystrokes and the detection of events in the browser’s host process.

Detecting User Events beyond Keystrokes A continuous mouse movement results in a sequence of events, each of which carrying information about the coordinates of the cursor’s trajectory. These events are issued with an inter-event delay of 8 ms, and the (empty) event listener operation blocks the loop for approx 0.1 ms. The particular frequency and duration of these events makes mouse movements (or similar actions, like scrolling) easy to spot with LoopScan, as seen in Figure 10.

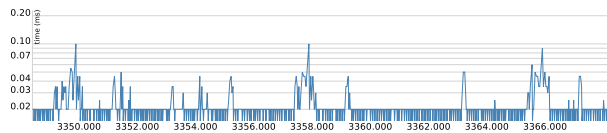


Figure 10: Mouse movement captured by LoopScan tool. The graph shows 3 delays of 0.1 ms duration (at t equals 3350, 3358 and 3366), with an inter-event delay of 8 ms.

Likewise, mouse click events, corresponding to “up” or “down”, can be identified using LoopScan. Their shape depends on the specific event listener of the spied web page and the HTML element being clicked. We expect that events *with* specific listeners are more easily detectable than events *without* registered event listeners, that is, user actions that do not trigger Javascript execution. However, we can use the context in which the event occurs to reduce the search space. For instance, most mouse clicks only appear between two sequences of mouse movement events.

We are currently investigating techniques that enable the automatic identification of such patterns in event-delay streams. A promising starting point for this are existing on-line variants of dynamic time-warping [31].

Detecting User Events in the Host Process Our discussion so far has centered on detecting user events in the event loop of the renderer process. However, all user events originate in the main thread of the host process and are sent towards a specific renderer through the event loop of the host’s I/O thread. Hence, any user action can in principle be detected by spying on the host.

Unfortunately, our current methods are not precise enough for this task, since the host’s I/O thread is more noisy than the renderer’s main thread and the effect of a user action on the host process is limited to a short signaling message, whereas the renderer’s main thread is

affected by the execution of the corresponding Javascript event listener.

4.3 Covert Channel

In this section we show how shared event loops in Chrome can be abused for implementing covert channels, i.e. channels for illicit communication across origins. We first consider the case of cross-origin pages sharing the event loop of a renderer’s main thread before we turn to the case of cross-origin pages sharing the event loop of the host processes’ I/O thread.

4.3.1 Renderer Process

We implement a communication channel to transmit messages from a sender page S to a cross-origin receiver page R running in the same renderer process.

For this, we use a simple, unidirectional transmission scheme without error correction. Specifically, we encode each bit using a time interval of fixed duration t_b . The optimal configuration of t_b depends on the system. In our experiments we tried different values, with $t_b = 5$ ms giving good results on different platforms: Chromium 52.0 on Debian 64-bit and Chrome 53 on OSX.

In each of those intervals we do the following:

- the sender S idles for transmitting a 0; it executes a blocking task of duration $\hat{t} < t_b$ for transmitting a 1.
- the receiver R monitors the event loop of the renderer’s main thread using the techniques described in Section 3.1; it decodes a 0 if the length of the observed tasks is below a threshold (related to \hat{t}), and a 1 otherwise.

Transmission starts with S sending a 1, which is used by the agents to synchronize their clocks and start counting time intervals. Transmission ends with S sending a null byte. With this basic scheme we achieve rates of 200 *bit/s*. These numbers can likely be significantly improved by using more sophisticated coding schemes with error correction mechanisms; here, we are only interested in the proof-of-concept.

We note that there are a number of alternative covert channels for transmitting information between pages running in the same renderer [1], e.g., using `window.name`, `location.hash`, `history.length`, `scrollbar’s position` or `window.frames.length`. What distinguishes the event-loop based channel is that it does not require the sender and receiver to be connected, i.e. they do not need to hold references to each other in order to communicate.

4.3.2 Host Process

We also implement a communication channel to transmit messages between two cooperative renderer processes

sharing the host process. Transmission is unidirectional from sender S to receiver R . Figure 11 visualizes how this channel can be used, even if one of the parties browses in Incognito mode.

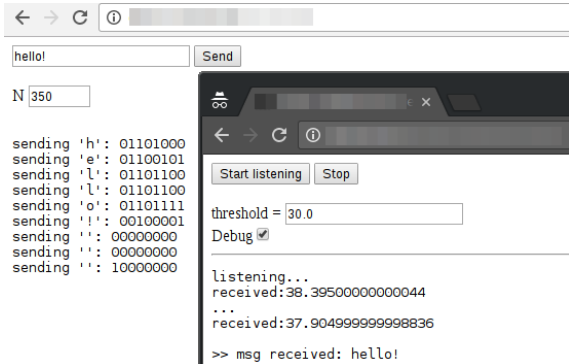


Figure 11: Covert channel through the I/O event loop of the Chrome’s host process. Tabs in different render processes (one of them navigating in *Incognito* mode) communicate.

As before, we encode each bit using a time intervals of fixed duration t_b . During each intervals we do the following:

- the sender S idles for transmitting a 0; it posts N fetch requests into the I/O thread’s queue for sending a 1.
- the receiver R monitors the event loop of the I/O thread of the host process using the techniques described in Section 3.2. It decodes a 0 if the number of observed events during time interval t_b is below a threshold, and 1 otherwise.

The optimal values of N and t_b highly depend on the machine. In our experiments we achieve good results, working on different systems, with a $t_b = 200$ ms and $N = 350$, which give us a 5 bit/s transmission rate. This rate is significantly lower than for communication using the renderer event loop, which is explained by the difference in noise and monitoring resolution of both channels, as discussed in Section 3.2.3.

The threat scenario of this covert channel is more relevant than the previous one for the renderer loop. For example it could be used for exfiltrating information from an attacked domain (on a tab executing malicious Javascript). Using Workers (which are background threads that run independently of the user interface) we can transfer information across origins, without affecting the user experience and without generating network traffic.

5 Discussion

We have shown how sharing event loops leads to timing side-channels and presented different attacks on Chrome. We communicated our findings to the Chromium security team, who decided not to take action for the time being. Nevertheless, our results point to fundamental security issues in the event-driven architecture of browsers that eventually need to be addressed in a fundamental manner. Below, we discuss how other platforms are affected and present possible countermeasures.

5.1 Beyond Chrome

We focus on Chrome in our analysis because it is the most widely used browser, and because it was the first one to implement a multi-process architecture. However, there are good reasons to expect similar side channels in other browsers, as they all follow the same event-driven paradigm and rely on similar architectures.

For instance, recent Firefox versions with multi-process support⁵ also rely on a privileged *browser process* and multiple *content processes* that, unlike renderers in Chrome, act as a pool of threads for each different origin (each with its own message queue). Despite this difference, tests with LoopScan on Firefox version 55 show that congestion on both event loops is observable across origins and tabs.

Specifically, we applied the monitoring technique for the renderers described in Section 3.1.2 on a micro-benchmark with a set of 30 pages with 15 traces each. We achieved a recognition rate of 49%, which is below the recognition rate achieved on Chrome for a set of 500 pages. A fair comparison between both architectures will require a better understanding of Firefox’s policy for mapping sites to threads and events to loops.

5.2 Countermeasures

The attacks presented in this paper rely on two capabilities of the adversary: (1) the ability to post tasks into the loop’s queue with high frequency, and (2) the ability to accurately measure the corresponding time differences.

Rate Limiting. An obvious approach to counter (1) is to impose a limit on the rate at which tasks can be posted into an event loop. Unfortunately, rate limiting implies penalties on performance, which is especially problematic for asynchronous code.

At the level of the renderer, one possibility is to rely on an *accumulate and serve* policy [22]. With this policy, the event loop accumulates all the incoming jobs

⁵Firefox’s Electrolysis (or e10s) project

in a buffer for a period T , and then process and serves all the accumulated jobs from party A , followed by all the jobs from V . This has the advantage of limiting the amount of information leaked while retaining high amortized throughput.

At the level of the host process, where resource fetching is one of the main performance concerns, setting any bound on the processing rate is not acceptable. Here, it seems more reasonable to monitor the IPC activity of all renderers and penalize or flag those who exhibit a bad or anomalous behavior, e.g., along the lines of [39].

Reduce Clock Resolution. An obvious approach to counter (2) is to limit the resolution of available clocks. This has already been applied by browser vendors for mitigating other kinds timing channels, but these efforts are unlikely to succeed, as shown in [23]: Modern browsers have a considerable number of methods to measure time without any explicit clock. For instance, some recent exploits [16] use high-resolution timers build on top of `SharedArrayBuffers`. The current resolution of `performance.now` is limited to $5\mu\text{s}$, which makes microarchitectural timing attacks difficult, but does not preclude the detection of Javascript events.

Full Isolation. As discussed in Section 2.2, Chrome’s multi-process architecture tries to use a different renderer for different origins, except for some corner cases. The “Site Isolation Project” is an ongoing effort to ensure a complete process-per-site-instance policy, that means: providing cross-process navigations, cross-process Javascript interactions and out-of-process iframes. All this without inducing too much overhead.

One open question is how to handle the system’s process limit, namely which sites should have isolation preference, or which heuristic for process reuse should be used. A recent proposal, “IsolateMe” [4], puts the developers in charge of requesting to be isolated from other web content (even if it does not provide a firm guarantee).

CPU Throttling. Chrome v55 introduces an API that allows to limit how much CPU a background page is allowed to use, and to throttle tasks when they exceed this limit. This affects background tabs trying to spy on the renderer’s main thread, but still allows spying on (and from) any iframe and popup, as well as on the I/O thread of the host process through shared Workers. Moreover, background tabs with audio activity are not affected, as they are always marked as foreground. Since Chrome v57 pages (or tabs) are only subjected to throttling after 10 seconds in the background, which is too long to prevent the attacks in this paper.

6 Related Work

Timing attacks on web browsers date back to Felten and Schneider [13], who use the browser cache to obtain information about a user’s browsing history.

More recently, so-called cross-site timing attacks [10, 35] have exploited the fact that the browser attaches cookies to all requests, even when they are performed across origins. The presence or absence of these cookies can be determined by timing measurements, which reveals information about the user’s state on arbitrary sites. A special case are cross-site search attacks [14], which circumvent the same-origin policy to extract sensitive information, by measuring the time it takes for the browser to receive responses to search queries.

Other classes of browser-based timing attacks exploit timing differences in rendering operations [24, 33, 5], or simply use the browser as an entry point for Javascript that exploits timing channels of underlying hardware, for example caches [26, 16], DRAM buffers [17], or CPU contention [9].

Of those approaches, [9] is related to our work in that it identifies web pages across browser tabs, based on timing of Javascript and a classifier using dynamic time warping. However, because the attack relies on CPU contention as a channel, it requires putting heavy load on all cores for monitoring. In contrast, our attack exploits the browser’s event loop as a channel, which can be monitored by enqueueing one event at a time. This makes our attack stealthy and more independent of the execution platform.

To the best of our knowledge, we are first to mount side-channel attacks that exploit the event-driven architecture of web browsers. Our work is inspired by a proof-of-concept attack [36] that steals a secret from a cross-origin web application by using the single-threadedness of Javascript. We identify Chrome’s event-driven architecture as the root cause of this attack, and we show how this observation generalizes, in three different attacks against two different event loops in Chrome.

Finally, a central difference between classical site fingerprinting [28, 19, 34, 12] approaches and our page identification attack is the adversary model: First, our adversary only requires its page to be opened in the victim’s browser. Second, instead of traffic patterns in the victim’s network, our adversary observes only time delays in the event queues of the victim’s browser. We believe that our preliminary results, with up to 76% of recognition rate using *one single* sample for training in a closed-world with 500 pages, can be significantly improved by developing domain-specific classification techniques.

7 Conclusions

In this paper we demonstrate that shared event loops in Chrome are vulnerable to side-channel attacks, where a spy process monitors the loop usage pattern of other processes by enqueueing tasks and measuring the time it takes for them to be dispatched. We systematically study how this channel can be used for different purposes, such as web page identification, user behavior detection, and covert communication.

Acknowledgments We thank Thorsten Holz, Andreas Rossberg, Carmela Troncoso, and the anonymous reviewers for their helpful comments. We thank Javier Prieto for his help with the data analysis. This work was supported by Ramón y Cajal grant RYC-2014-16766, Spanish projects TIN2012-39391-C04-01 StrongSoft and TIN2015-70713-R DEDETIS, and Madrid regional project S2013/ICE-2731 N-GREENS.

References

- [1] Covert channels in the sop. <https://github.com/cgvwzq/sop-covert-channels>. Accessed: 2017-02-16.
- [2] HTML Living Standard. <https://html.spec.whatwg.org/>. Accessed: 2017-05-24.
- [3] Understanding about:tracing results. <https://www.chromium.org/developers/how-tos/trace-event-profiling-tool/trace-event-reading>. Accessed: 2017-02-16.
- [4] Isolation explainer. <https://wicg.github.io/isolation/explainer.html>, 2016. Accessed: 2017-05-24.
- [5] ANDRYSCO, M., KOHLBRENNER, D., MOWERY, K., JHALA, R., LERNER, S., AND SHACHAM, H. On subnormal floating point and abnormal timing. In *SSP* (2015), IEEE.
- [6] BARTH, A., JACKSON, C., REIS, C., TEAM, T., ET AL. The security architecture of the chromium browser. <http://www.adambarth.com/papers/2008/barthjackson-reis.pdf>, 2008.
- [7] BERNDT, D. J., AND CLIFFORD, J. Using dynamic time warping to find patterns in time series. In *KDD workshop* (1994), AAAI Press.
- [8] BERNSTEIN, D. Cache-timing attacks on AES. <https://cr.yp.to/antiforgery/cachetiming-20050414.pdf>, 2005.
- [9] BOOTH, J. M. Not so incognito: Exploiting resource-based side channels in javascript engines. <http://nrs.harvard.edu/urn-3:HUL.InstRepos:17417578>, 2015.
- [10] BORTZ, A., AND BONEH, D. Exposing private information by timing web applications. In *WWW* (2007), ACM.
- [11] BOSMAN, E., RAZAVI, K., BOS, H., AND GIUFFRIDA, C. Dedup Est Machina: Memory Deduplication as an Advanced Exploitation Vector. In *SSP* (2016), IEEE.
- [12] DYER, K. P., COULL, S. E., RISTENPART, T., AND SHRIMP-TON, T. Peek-a-Boo, I Still See You: Why Efficient Traffic Analysis Countermeasures Fail. In *SSP* (2012), IEEE.
- [13] FELTEN, E. W., AND SCHNEIDER, M. A. Timing attacks on web privacy. In *CCS* (2000), ACM.
- [14] GELERNTER, N., AND HERZBERG, A. Cross-Site Search Attacks. In *CCS* (2015), ACM.
- [15] GIORGINO, T. Computing and visualizing dynamic time warping alignments in r: The dtw package. *JSS* 31, 7 (2009), 1–24.
- [16] GRAS, B., RAZAVI, K., BOSMAN, E., BOS, H., AND GIUFFRIDA, C. ASLR on the Line: Practical Cache Attacks on the MMU. In *NDSS* (2017), The Internet Society.
- [17] GRUSS, D., MAURICE, C., AND MANGARD, S. Rowhammer.js: A remote software-induced fault attack in javascript. In *DIMVA* (2016), Springer.
- [18] GRUSS, D., SPREITZER, R., AND MANGARD, S. Cache template attacks: Automating attacks on inclusive last-level caches. In *USENIX Security* (2015), USENIX Association.
- [19] HAYES, J., AND DANEZIS, G. k-fingerprinting: A Robust Scalable Website Fingerprinting Technique. In *USENIX Security* (2016), USENIX Association.
- [20] HOGYE, M. A., HUGHES, C. T., SARFATY, J. M., AND WOLF, J. D. Analysis of the feasibility of keystroke timing attacks over ssh connections. <http://www.cs.virginia.edu/~evans/cs588-fall12001/projects/reports/team4.pdf>, 2001.
- [21] JANA, S., AND SHMATIKOV, V. Memento: Learning secrets from process footprints. In *SSP* (2012), IEEE.
- [22] KADLOOR, S., KIYAVASH, N., AND VENKITASUBRAMANIAM, P. Mitigating timing side channel in shared schedulers. *IEEE/ACM Trans. Netw.* 24, 3 (2016), 1562–1573.
- [23] KOHLBRENNER, D., AND SHACHAM, H. Trusted Browsers for Uncertain Times. In *USENIX Security* (2016), USENIX Association.
- [24] KOTCHER, R., PEI, Y., JUMDE, P., AND JACKSON, C. Cross-origin pixel stealing: timing attacks using CSS filters. In *CCS* (2013), ACM.
- [25] LAMPSON, B. W. A note on the confinement problem. *Communications of the ACM* 16, 10 (1973), 613–615.
- [26] OREN, Y., KEMERLIS, V. P., SETHUMADHAVAN, S., AND KEROMYTIS, A. D. The Spy in the Sandbox: Practical Cache Attacks in JavaScript and Their Implications. In *CCS* (2015), ACM.
- [27] OSVIK, D. A., SHAMIR, A., AND TROMER, E. Cache attacks and countermeasures: the case of AES. In *CT-RSA* (2006), Springer.
- [28] PANCHENKO, A., LANZE, F., PENNEKAMP, J., ENGEL, T., ZINNEN, A., HENZE, M., AND WEHRLE, K. Website fingerprinting at internet scale. In *NDSS* (2016), The Internet Society.
- [29] PEDERSEN, M. V., AND ASKAROV, A. From Trash to Treasure: Timing-sensitive Garbage Collection. In *SSP* (2017), IEEE.
- [30] REIS, C., AND GRIBBLE, S. D. Isolating web programs in modern browser architectures. In *EuroSys* (2009), ACM.
- [31] SAKURAI, Y., FALOUTSOS, C., AND YAMAMURO, M. Stream monitoring under the time warping distance. In *ICDE* (2007), IEEE.
- [32] SONG, D. X., WAGNER, D., AND TIAN, X. Timing Analysis of Keystrokes and Timing Attacks on SSH. In *USENIX Security* (2001), USENIX Association.
- [33] STONE, P. Pixel perfect timing attacks with html5 (white paper). https://www.contextis.com/documents/2/Browser_Timing_Attacks.pdf, 2013.
- [34] SUN, Q., SIMON, D. R., WANG, Y.-M., RUSSELL, W., PADMANABHAN, V. N., AND QIU, L. Statistical identification of encrypted web browsing traffic. In *SSP* (2002), IEEE.
- [35] VAN GOETHEM, T., JOOSEN, W., AND NIKIFORAKIS, N. The Clock is Still Ticking: Timing Attacks in the Modern Web. In *CCS* (2015), ACM.

- [36] VELA, E. Matryoshka: Timing attacks against javascript applications in browsers. <http://sirdarckcat.blogspot.com.es/2014/05/matryoshka-web-application-timing.html>, 2013.
- [37] YAROM, Y., AND FALKNER, K. FLUSH+RELOAD: A high resolution, low noise, L3 cache side-channel attack. In *USENIX Security Symposium* (2014).
- [38] ZHANG, K., AND WANG, X. Peeping tom in the neighborhood: Keystroke eavesdropping on multi-user systems. In *USENIX Security* (2009), USENIX Association.
- [39] ZHANG, T., ZHANG, Y., AND LEE, R. B. CloudRadar: A Real-Time Side-Channel Attack Detection System in Clouds. In *RAID* (2016), Springer.